Sensors & Transducers, Vol. 166, Issue 3, March 2014, pp. 203-212

www.sensorsportal.com

Sensors & Transducers

http://www.sensorsportal.com

Passive ISAR Imaging Using Multi-channel DVB-T Signals

Kaiwang Lu, Jie Yang, Xiaoqing Qi and Liangjun Zhang
Key Laboratory of Fiber Optic Sensing Technology and Information Processing,
Wuhan University of Technology, Ministry of Education, Wuhan, 430070, China
Tel.: 86-027-87290336
E-mail: xminforever@163.com

Received: 20 December 2013 /Accepted: 28 February 2014 /Published: 31 March 2014

Abstract: This paper analysis the characteristics and ambiguity function of the single-channel and multi-channel DVB-T signals, and choose the multi-channel DVB-T signal as opportunity illuminators to do the research of ISAR imaging. Firstly, the target's echo using single-in-multi-out mode for passive ISAR image is derived, together with the analysis of the composition of the echo's spatial spectrum. Considering the characteristic of the imaging model, PR-CLEAN method is given, which uses the CLEAN algorithm to extract the scatters from every received echoes after the Polar Reformatting algorithm is processed. The PR-CLEAN method can get better performance for noise suppression which caused by the Polar Reformatting algorithm, and improve imaging quality. Simulation results agree well with the theoretical analysis, and PR-CLEAN method is proved to be a good method for ISAR imaging in single-in-multi-out mode based on the multi-channel DVB-T signals. *Copyright © 2014 IFSA Publishing, S. L.*

Keywords: Multi-channel DVB-T, Polar reformatting algorithm, CLEAN algorithm, passive, ISAR.

1. Introduction

Passive radar system based on external illuminator (including broadcast, television, cellphone, etc) has been widely researched by many military powers because of its good "four resistances" characteristics. There are broad application prospects using passive radar receiver to implement target positioning, speed detection, recognition, even imaging and so on. However, in the passive radar system using external illuminators, most researches focus on target detection, while in radar imaging, enough bandwidth is needed to complete imaging of scattering points on targets. References [1-3] aimed at targets detection using FM signal as external illuminator and the design of matched filter for TV-based passive bistatic radar is introduced in [4,5]. With the development of ISAR technologies and the increase of bandwidth of commercial signals, target imaging methods based on external illuminators are studied further. Reference [6, 7] suggests that ISDB-T digital signal can be used to improve range resolution of ISAR imaging. To further improve the resolution of passive radar imaging, [8] and [9] firstly proposed multi-channel DVB-T signals. They studied the resolution performance of bistatic ISAR imaging based on multi-channel DVB-T signals and the signal processing methods. Reference [10] presented the polar reformatting algorithm methods to achieve target imaging in the mode of single illuminator and multiple receivers. But, when external illuminator is applied to imaging, a long-time integration is needed to improve its directional resolution, for example, by increasing the target's turn angle. In the polar coordinate, the interpolation method has to be used

when doing Fourier transform in order to form a target's 2D image. However, the noise made by interpolation method will cause the image ambiguous which makes it insufficient to use the polar coordinate reconstruction algorithm only in passive radar imaging.

This paper studies the multi-channel DVB-T signal and proposes the ISAR imaging methods in the mode of signal illuminator and multiple receivers based on multi-channel DVB-T signal using PR-CLEAN method. The remainder of this paper is organized as follows. Section 2 provides signal analysis of DVB-T signals, and Section 3 gives the echo signal model. Section 4 introduces the specific imaging method, including the polar coordinates reconstruction algorithm and improved CLEAN method. Simulation results are given in section 5. Section 6 concludes this paper.

2. Signal Analysis of DVB-T

In normal conditions, commercial signals are taken as the external illuminators, which is completely different from the general radar signals. Multi-band DVB-T signals are used to do the ISAR imaging in this paper. However, the signal and its ambiguity function need to be detailed analyzed beforehand.

2.1. Single / Multi-Band DVB-T Signal

DVB-T signal takes the OFDM method to do the modulation, which can be described as follows:

$$x(t)=e^{2j\pi f_0 t}\sum_{p=0}^{P-1}\sum_{q=0}^{Q-1}\sum_{r=0}^{N_{sc}-1}x_{p,q,r}\cdot\Psi_{p,q,r}(t) \tag{1}$$

where f_0 is the carrier frequency, P is the number of transmitted frames, Q is the number of symbols in each frame, N_{sc} is the number of carriers in each symbol, $x_{p,q,r}$ is the parallel symbols, and

$$\Psi_{p,q,r}(t)=\begin{cases}e^{2j\pi\frac{r}{Tu}(t-T_0-(pQ+q)T_s)} & (pQ+q)T_s\le T\le(pQ+q+1)T_s\\ 0 & others\end{cases} \tag{2}$$

DVB-T signal is a kind of multicarrier signal constituted by numbers of carriers, which has two modes (2K and 8K). Besides, 2K and 8K mode corresponding to 1705 carriers and 6817 carriers respectively. In this paper, 2K mode is taken to do the research.

In (1), set $\tilde{s}_m(t)=\sum_{p=0}^{P-1}\sum_{q=0}^{Q-1}\sum_{r=0}^{N_{sc}-1}x_{p,q,r}\cdot\Psi_{p,q,r}(t)$, so that the multi-band DVB-T signal can be expressed as

$$s(t)=\mathrm{Re}\left\{\sum_{m=0}^{N_c-1}\tilde{s}_m(t)e^{j2\pi f_m t}\right\} \tag{3}$$

where N_c is the number of the television band, f_m is the carrier frequency of the m th band, $\tilde{s}_m(t)$ is the band of the m th complex envelope. Suppose N_c bands are evenly spaced, then $f_m=f_0+m\cdot\Delta f$, and Δf refers to the bandwidth of each band.

Fig. 1 (a) shows the time domain signal of single-band DVB-T with one symbol, and its spectrum is shown in Fig. 1(b). The DVB-T time-domain signal with 8 adjacent frequencies is shown in Fig. 2 (a), and the spectrum is shown in Fig. 2 (b).

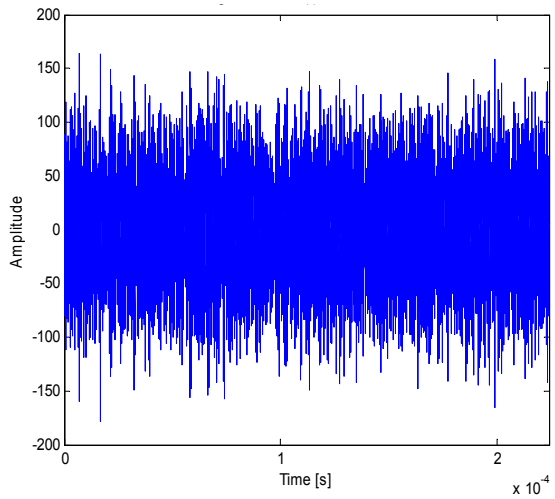

(a) Time-domain

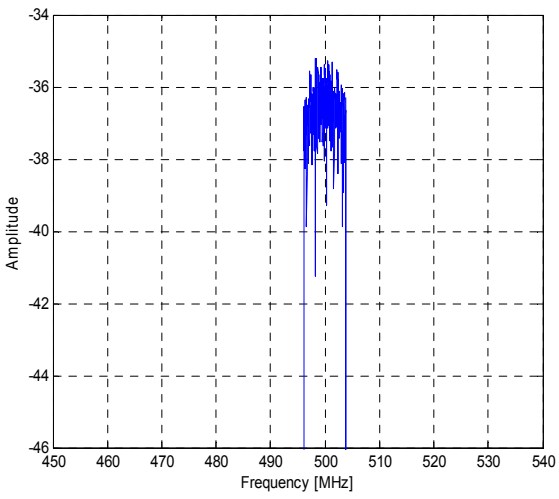

(b) Frequency-domain

Fig. 1. Single-channel DVB-T signal.

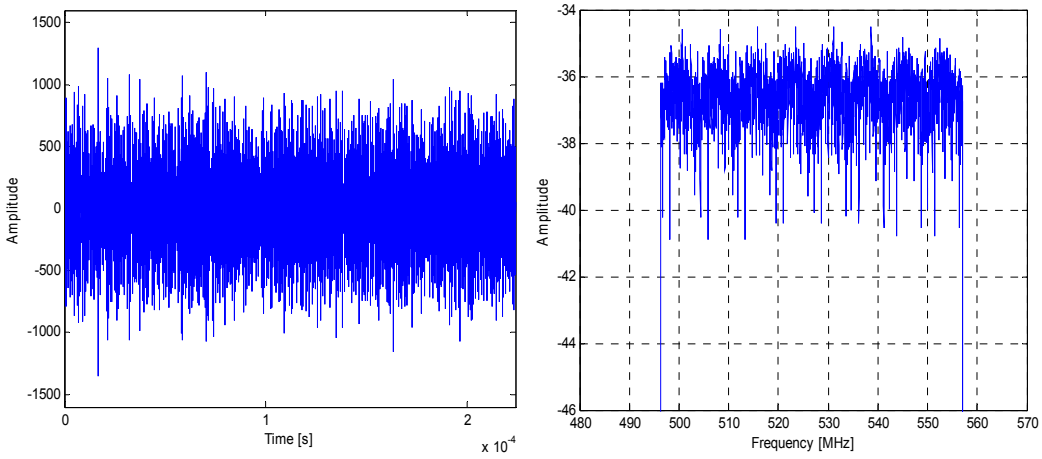

(a) Time-domain (b) Frequency-domain

Fig. 2. 8-channel DVB-T signal.

From the figures we can see that there is no difference in transmitting between single-channel and multi-channel DVB-T signals, while the amplitude of multi-channel signal is enhanced compared to the single-channel signal. This is because it uses 8 channels for transmission of a symbol in the same digital signal, which leads to the signal intensity increased by 8 times. Besides, it is obvious that the bandwidth of multi-channel signal is larger than that of single-channel signal.

2.2. Ambiguity Function Analysis of DVB-T Signals

The ambiguity function of radar signal is an important function, which is used to judge the resolution of target positioning and speed measuring. It is defined as the following equation:

$$\chi(\tau, f_d) = \left| \int_{-\infty}^{+\infty} S(t) S^*(t-\tau) e^{j2\pi f_d t} dt \right|^2, \quad (4)$$

where $S(t)$ is the radar signal, τ is the time delay, namely the distance of radar, and f_d is the Doppler frequency, which corresponds to the speed of target.

The ambiguity function of the radar signal can help to analysis the radar signal and design the waveform. Besides, it can judge the waveform of signal, and the performance index such as target resolution, velocity-measuring ability, measuring accuracy and ground clutter suppression and so on. Even if passive bistatic (multistatic) radar system is different from monostatic radar system in target detecting, the parameter evaluation, clutter interference, and signal detection etc. of passive radar can also be measured by the ambiguity function of the external illuminators. From the above analysis we can know the analysis and research of signals' ambiguity function is the theoretical basis for external illuminator selecting in passive radar system. Fig. 3 and Fig. 4 show the ambiguity functions of single-channel DVB-T signal and 8-channel DVB-T signal.

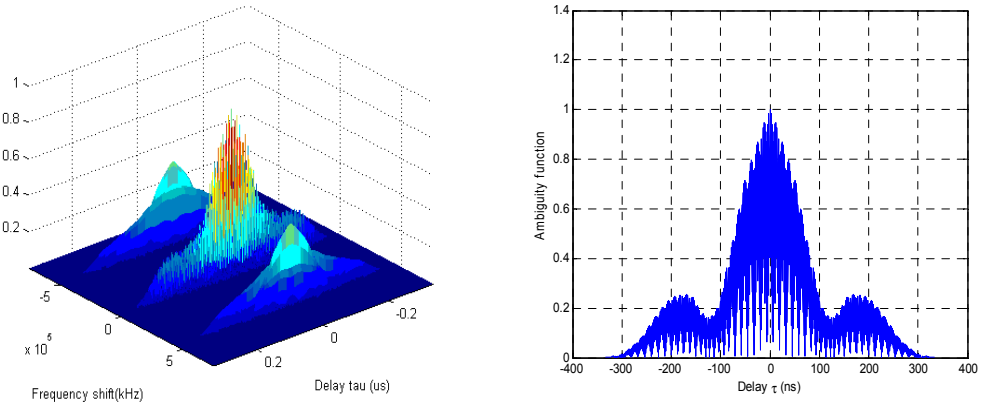

(a) Ambiguity Function (b) Autocorrelation Function

Fig. 3. Single-channel DVB-T signals.

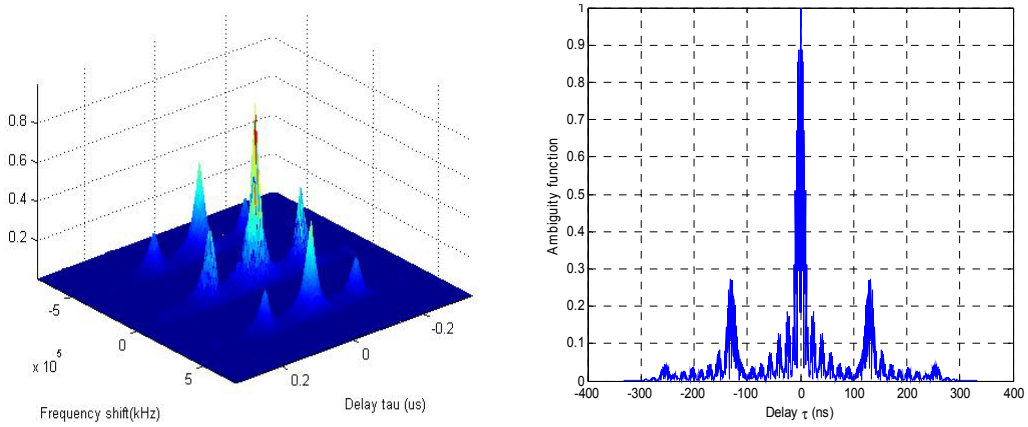

(a) Ambiguity Function (b) Autocorrelation Function

Fig. 4. 8-channel DVB-T signal.

Compare the ambiguity function shown in Fig. 3(a) and Fig. 4(a), it is clear that 8-channel DVB-T signal is significantly better than the single-band DVB-T signal. 8-channel DVB-T signal looks more like a thumbtack shape, which means it has better velocity and range resolution. Analysis the autocorrelation function in Fig. 3(b) and Fig. 4(b), similar conclusion can be get, 8-channel signal has improved range resolution than single-band signal.

3. Echo Signal Model

This paper studies the single-emission and multi-receiving mode imaging, the system model is shown in Fig. 5. The DVB basestation is located in T, establish the $x-y$ coordinate system, the i th receiver is placed at R_i, and also establish the $x-y$ coordinate system. Differently, establish u–v system at the target's rotation center. The distances between target and basestation and receiver is denoted by $R_T(t)$ and $R_{iR}(t)$ respectively, with unit vectors $\vec{t}$ and $\vec{r}_i$. The arbitrary scattering point P on the target has the polar coordinate (r_p, θ) in the target $x-y$ coordinate system, with the unit vector $\vec{r}_p$. At any time t, the distance between P and basestation is $R_t(t)$, while the distance between P and receiver is $R_{ir}(t)$. The parameter β_i denotes the bistatic angle between basestation and i th receiver.

The multi-channel DVB-T signal is written as $s(t)=\mathrm{Re}\left\{\sum_{m=0}^{N_c-1}\tilde{s}_m(t)e^{j2\pi f_m t}\right\}$, which is used to generate the target echo signals in the following sections. According to the point scatterer model, the echo signal received at i th receiver reflected from scatter point P can be written as

$$s_{ir}(t)=s\left(t-\tau_p\right) \tag{5}$$

where $\tau_p=\frac{R_t(t)+R_{r_i}(t)}{c}$, which means the time delay for the signal transmit from scatterer P to the receiver at time t. $R_t(t)$ is the distance between scattering point and TV basestation, and $R_{ir}(t)$ is the distance between scattering point and receiver.

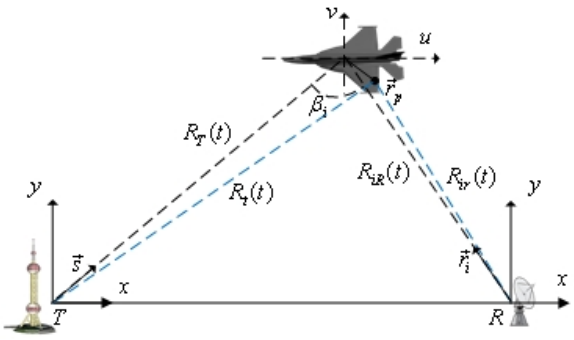

Fig. 5. Bistatic ISAR imaging model.

By means of the theory of diffraction geometry GDT, (5) can be changed to

$$s_{ir}(w)=s(w)\exp\left(-jw\tau_p\right) \tag{6}$$

where $s_{ir}(w)$ is the i th received echo in frequency domain, and $s(w)$ is the transmitted signal in frequency domain, $w=2\pi f$. Diffraction geometrical theory GDT is originally obtained in the frequency domain, so apply Fourier transform on both sides of (5). Then, (6) can be derived with the help of diffraction theory, which can be written as

$$s_{ir}(f)=s(f)\exp\left(-j2\pi f\frac{R_t(t)+R_{ir}(t)}{c}\right) \tag{7}$$

where

$$\begin{cases} R_t(t) = \left| R_T(t) \cdot \vec{s} + \vec{r}_p \right| \cong R_T(t) + \vec{s} \cdot \vec{r}_p \\ R_{ir}(t) = \left| R_{iR}(t) \cdot \vec{r}_i + \vec{r}_p \right| \cong R_{iR}(t) + \vec{r}_i \cdot \vec{r}_p \end{cases} \tag{8}$$

Assuming that the scattering amplitude of target point is 1, the whole target echoes is

$$s_{ir}(f) = s(f) \sum_{p=1}^{Num} \exp\left(-j2\pi f \frac{R_t(t) + R_{ir}(t)}{c} \right) \tag{9}$$

Apply (8) to (9)

$$s_{ir}(f) = s(f) \sum_{p=1}^{Num} \exp\left(-j2\pi f \frac{R_T(t) + R_{Ri}(t)}{c} \right) \cdot \exp\left(-j2\pi f \frac{(\vec{s} + \vec{r}_i) \cdot \vec{r}_p}{c} \right) \tag{10}$$

where *Num* is the number of scatter points on the target.

After applying matched filter, (10) changed to

$$\begin{aligned} S_{iR}(f) &= \frac{s_{ir}(f)}{s(f)} \\ &= \exp\left(-j2\pi f \frac{R_T(t) + R_{iR}(t)}{c} \right) \sum_{p=1}^{Num} \exp\left(-j2\pi f \frac{(\vec{s} + \vec{r}_i) \cdot \vec{r}_p}{c} \right) \end{aligned} \tag{11}$$

where $R_T(t)$ and $R_{iR}(t)$ are the functions of slow time. When the transmitted pulse is relatively short, $R_T(t)$ and $R_{iR}(t)$ can be regard as approximate constant in the duration of the pulse, which can also be written as $R_T(t_m)$ and $R_{iR}(t_m)$. t_m is the slow time of each pulse. In the same pulse, apply N-point sampling in the frequency domain, we can get

$$S_R(f_n, t_m, i) = \exp\left(-j2\pi f_n \frac{R_T(t_m) + R_{iR}(t_m)}{c} \right) \sum_{p=1}^{Num} \exp\left(-j2\pi f_n \frac{(\vec{s} + \vec{r}_i) \cdot \vec{r}_p(t_m)}{c} \right) \tag{12}$$

In (12), $\exp\left(-j2\pi f_n \frac{R_T(t_m) + R_{iR}(t_m)}{c} \right)$ part is removed after doing range compression and motion compensation, which can result in achieved high range resolution. The signal's spectrum may be expressed as

$$S_0(f_n, t_m, i) = \sum_{p=1}^{Num} \exp\left(-j2\pi f_n \frac{(\vec{s} + \vec{r}_i) \cdot \vec{r}_p(t_m)}{c} \right) \tag{13}$$

$S_0(f_n, t_m, i)$ are the transmitted electromagnetic waves with frequencies of f_n $(n = 1, 2, 3 \ldots N)$ in the direction of $\vec{s}$ in different slow time slots. The i^{th} receiver receives scattering echo from the direction of $\vec{r}_i$. Suppose that the target rotates counterclockwise uniformly at the angular velocity of w around a reference point, then

$$\begin{cases} \vec{s} \cdot \vec{r}_p(t_m) = r_p \sin\left(\theta + \frac{\beta_i}{2} + wt_m \right) \\ \vec{r}_i \cdot \vec{r}_p(t_m) = r_p \sin\left(\theta - \frac{\beta_i}{2} + wt_m \right) \end{cases} \tag{14}$$

Substitute (14) into (13), then

$$S_0(f_n, t_m, i) = \sum_{p=1}^{Num} \exp\left(-j2\pi f_n \frac{r_p \left(\sin\left(\theta + \frac{\beta_i}{2} + wt_m \right) + \sin\left(\theta - \frac{\beta_i}{2} + wt_m \right) \right)}{c} \right) \tag{15}$$

Considering that $\begin{cases} x_p = r_p \cos(\theta) \\ y_p = r_p \sin(\theta) \end{cases}$, a new form of expression can be getting after triangular transformation:

$$S_0(f_n, t_m, i) = \sum_{p=1}^{Num} \exp\left(-j2\pi \frac{f_n}{c} \left(\begin{array}{l} x_p \left(\sin\left(\frac{\beta_i}{2} + wt_m \right) + \sin\left(-\frac{\beta_i}{2} + wt_m \right) \right) \\ + y_p \left(\cos\left(\frac{\beta_i}{2} + wt_m \right) + \cos\left(-\frac{\beta_i}{2} + wt_m \right) \right) \end{array} \right) \right) \tag{16}$$

After simplification, (16) becomes as follows

$$S_0(f_n, t_m, i) = \sum_{p=1}^{Num} \exp\left(-j2\pi \left(2\cos\frac{\beta_i}{2} \right) \frac{f_n}{c} \left(x_p \cdot \sin(wt_m) + y_p \cos(wt_m) \right) \right) \tag{17}$$

4. Proposed Imaging Algorithm

In previous sections, the spatial spectrum distribution of the bistatic ISAR is analyzed which is composed of single receiver and TV transmitting tower in polar coordinates. Interpolation processing on the spatial spectrum distribution needs to be done before applying Fourier transformation to get the spectral estimation. By doing interpolation, the uneven points of the echo become uniform distributed, so that we can conduct the spectral estimation using the Fourier transformation. However, interpolation process brings noises when using the polar coordinate reconstruction algorithm. Besides, the number of false scattering points increases, and all the factors result in a blurred image. To avoid the effect of noise and false points, CLEAN method is proposed to filter the interferences and improve the quality of imaging.

4.1 Polar Coordinates Reconstruction

The target direction of X and Y correspond to azimuth and distance respectively. When $\beta = 0^\circ$, equation (17) becomes the spatial spectral density function of monostatic radar imaging. The spatial spectrum of monostatic is

$$\begin{cases} f_n^x = f_n \cdot \sin(wt_m) \\ f_n^y = f_n \cdot \cos(wt_m) \end{cases} \tag{18}$$

In bistatic radar system, the spatial spectrum is

$$\begin{cases} f_n^x = \cos\dfrac{\beta_i}{2} f_n \cdot \sin(wt_m) \\ f_n^y = \cos\dfrac{\beta_i}{2} f_n \cdot \cos(wt_m) \end{cases} \tag{19}$$

Fig. 6 describes the compositions of the spatial spectrum of monostatic and bistatic system. It shows the diagrammatic sketch of the spatial spectrum generated by basestation and i th receiver. Compared with the monostatic system, the spatial spectrum of bistatic system reduced to $\cos(\beta_i/2)$ because of the effect of $\cos(\beta_i/2)$ factor.

Besides, Fig. 6 shows that the polar form of echo looks not like a rectangular shape in the space. So if we want to conduct Fourier transformation, interpolation processing needs to be done which can convert polar coordinates to rectangular coordinates. Carry out four-point interpolation for each received echo, just like Fig. 7.

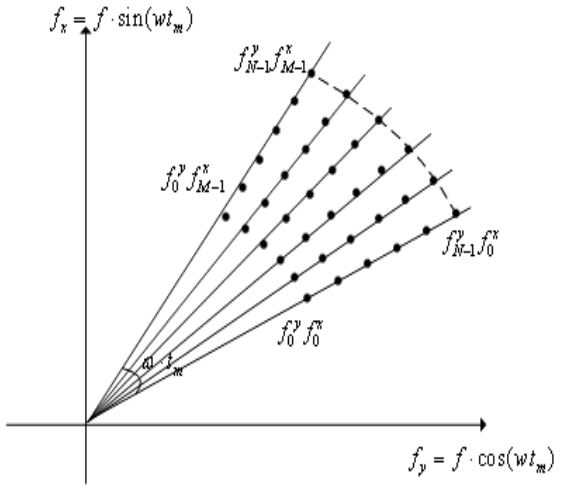

(a) Monostatic

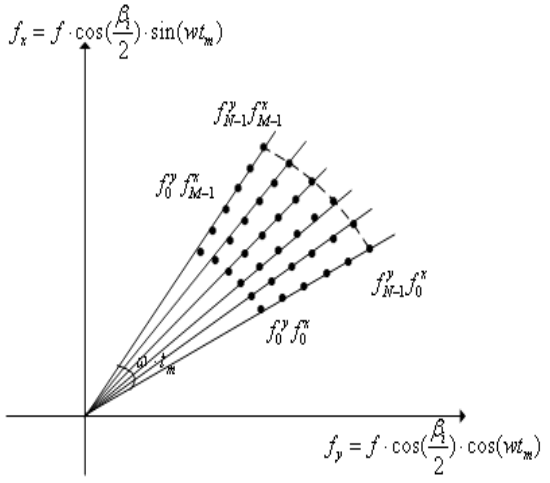

(b) Bistatic

Fig. 6. Composition of spatial spectrum.

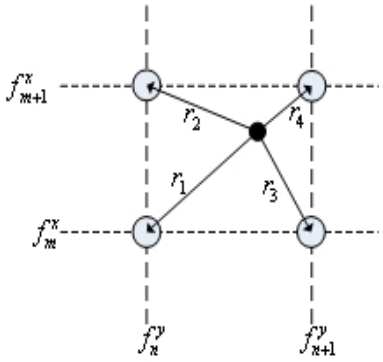

(a) Four-point interpolation

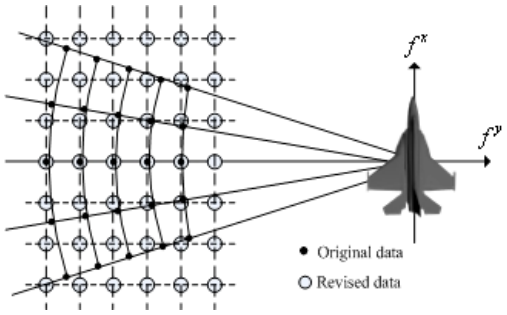

(b) Points after interpolation

Fig. 7. Interpolation in polar coordinates.

Set the echo amplitude with A_i, the four most adjacent points between the four points ($\left[f_n^y, f_m^x\right]$, $\left[f_n^y, f_{m+1}^x\right]$, $\left[f_{n+1}^y, f_m^x\right]$ and $\left[f_{n+1}^y, f_{m+1}^x\right]$) can be expressed using the point echo in the plane as in (19):

$$\begin{aligned} \widetilde{S}_i\left[f_n^y, f_m^x\right] &= A_i \cdot \frac{R}{r_1} \qquad \widetilde{S}_i\left[f_n^y, f_{m+1}^x\right] = A_i \cdot \frac{R}{r_2} \\ \widetilde{S}_i\left[f_{n+1}^y, f_m^x\right] &= A_i \cdot \frac{R}{r_3} \qquad \widetilde{S}_i\left[f_{n+1}^y, f_{m+1}^x\right] = A_i \cdot \frac{R}{r_4}, \end{aligned} \tag{20}$$

where $R = \dfrac{1}{1/r_1 + 1/r_2 + 1/r_3 + 1/r_4}$, and $r_k\ (k = 1,2,3,4)$ represents the distance between the point and its nearest point. After the interpolation, the spectrum of echo evenly spaced in the rectangular coordinate system, see Fig. 7. Next, we can carry out the Fourier transformation directly to do the spectrum estimation and obtain the two-dimensional image of target.

4.2. Conventional CLEAN Algorithm

In polar coordinates system, ISAR imaging can be described as a two-dimensional convolution process between target scattering point and point spread functions. It will cause false target and reduce the quality of imaging seriously because the convolution process will produce strong sidelobes. CLEAN algorithm can be regarded as a deconvolution

process, or a filtering process. In the CLEAN algorithm, the image residual after n th iteration can be written as

$$\begin{bmatrix} 2D\ residual \\ image \end{bmatrix}^{n} = \begin{bmatrix} 2D\ residual \\ image \end{bmatrix}^{n-1} - A_n \cdot h(x-x_n, y-y_n), \quad (21)$$

where A_n is the strongest point located at (x_n, y_n). That is, the image residual after n th iteration equals to the $(n-1)$ th iteration residual minus the point scattering function of the strongest point in the $(n-1)$ th iteration. The specific CLEAN algorithm is introduced in Algorithm 1. We can extract the scattering point position and amplitude information by adopting CLEAN algorithm using the target echo.

Algorithm 1. CLEAN algorithm.

Step 1: Find the point with maximum amplitude, denoted by $A_{\max}$, locates at (x_i, y_i).

Step 2: Generate the point scattering function $B(x, y)$ as the reference, and move the center of the reference function to (x_i, y_i), get the result of $A_{\max} \cdot B(x-x_i, y-y_i)$.

Step 3: Subtract the calculated result in previous step from the original data and rebuild the image residual.

Step 4: Go back to step 1 and repeat the above operation until all the points are found or the signal closes to the noise level.

Step 5: Construct the "clean" image using calculated amplitude $A_{\max}$ and the corresponding position (x_i, y_i) in the iterative process.

4.3. Proposed PR-CLEAN Method

Because of the multiple noises produced in Polar coordinate interpolation reconstruction algorithm, the image usually blur seriously. In order to improve the quality of imaging, this paper proposes the PR-CLEAN method, which uses CLEAN technology after Polar coordinate reconstruction algorithm, to filter the "dirty" image and extract the scattering center point. The specific ISAR imaging process using PR-CLEAN can be described in Algorithm 2.

Algorithm 2. PR-CLEAN algorithm.

Step 1: Preprocessing the received echoes of all the receiver, including mixing, pulse compression and motion compensation;

Step 2: Carry out polar coordinate reconstruction of the preprocessed echo and interpolate in the direction of range and azimuth. Four-point interpolation is used;

Step 3: Superposition all the signals after interpolation to get the original "dirty" image;

Step 4: Apply CLEAN method to the "dirty" image, then obtain the position and amplitude information of scattering points;

Step 5: Imaging the target using the position and the amplitude information produced in step 4.

Fig. 8 shows the complete ISAR process using PR-CLEAN method in single transmitter and multiple receivers' mode.

5. Simulation and Results

Simulation model is set up as Fig. 9. Establish the x-y coordinate system using the target reference point. Digital TV transmission tower is fixed on the positive side of y-axis, and locates at $S_t(r_0, 0)$. N receivers in Fig. 9(a) distribute on the coordinates in a clockwise direction with coordinates $S_i(r_i, \beta_i), i = 1, 2, \cdots, N$. And the interval between the receivers is $\Delta\beta$. The target goes around the reference point with the angle speed of φ.

Select the DVB-T signal with single frequency bandwidth $B = 7.6116\ MHz$, carrier frequency $f_c = 500\ MHz$, the target scattering points is generated as Fig. 9(b).

The rotation angle of target is set to $\varphi = 15^\circ$, the angle between the adjacent receivers is $\Delta\beta = 6^\circ$, the number of receivers is $N = 10$. Fig. 10 shows the imaging results using the polar coordinate reconstruction algorithm directly with the help of four-point interpolation, and the signals chose the 1, 3, 6 and 9 channels respectively.

Ensure all the parameters unchanged, using PR-CLEAN imaging algorithm to do the simulation again, the new results is shown in Fig. 11.

It can be seen from Fig. 10 and Fig. 11 that the imaging resolution gradually increases with the increase of DVB-T signal's frequency bands. It is because that the relationship between range resolution and bandwidth satisfies $\rho_a = \frac{c}{2B\cos(\beta/2)}$. In the equation, c is the speed of light, B is the bandwidth, and β is the bistatic angle between each receiver and the television transmission tower. Clearly, increase of the parameter B results in lesser ρ_a, which means higher range resolution. It can be seen from Fig. 11 that the DVB-T signal can imaging the target using polar reconstruction algorithm based on multi-band DVB-T signals in the single transmitter and multi receivers mode. However, the target images are blurred because of the interpolation operation in range and azimuth directions, which generates the noises and reduces the precision of image. After applying the proposed PR-CLEAN algorithm can filter the echo effectively after polar coordinate reconstruction and extract scatter centers together with denoising. Fig. 11 reveals that the imaging results after PR-CLEAN is significantly superior to conventional polar coordinates reconstruction imaging.

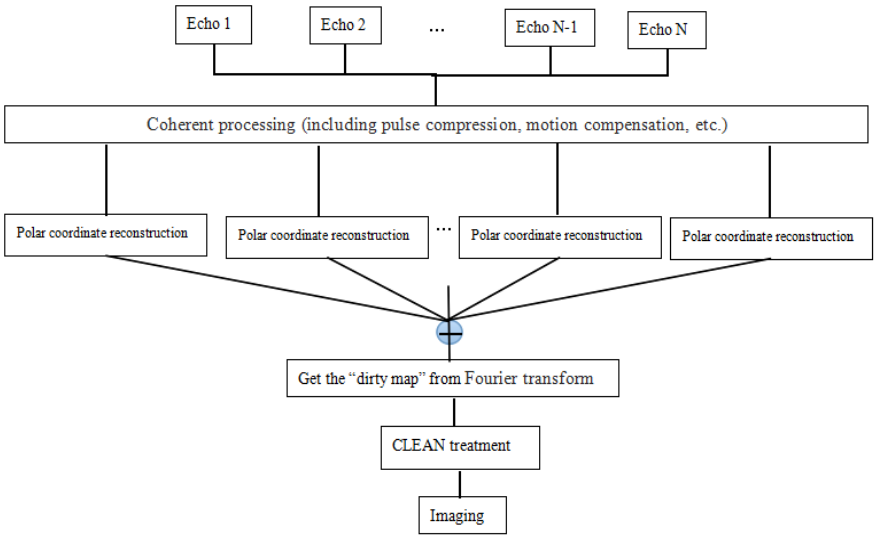

Fig. 8. ISAR process using PR-CLEAN method.

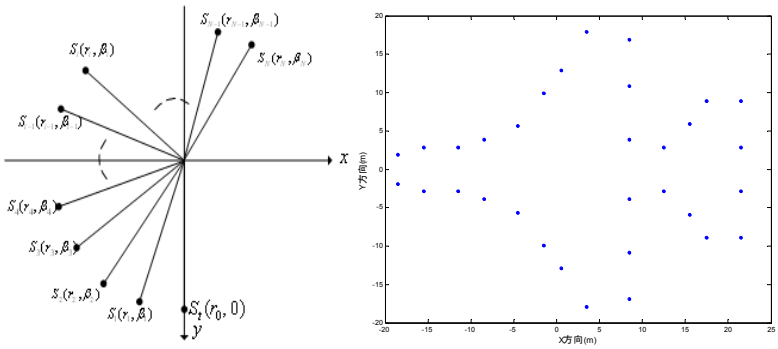

(a) Location of receivers (b) Target scattering point

Fig. 9. System simulation model.

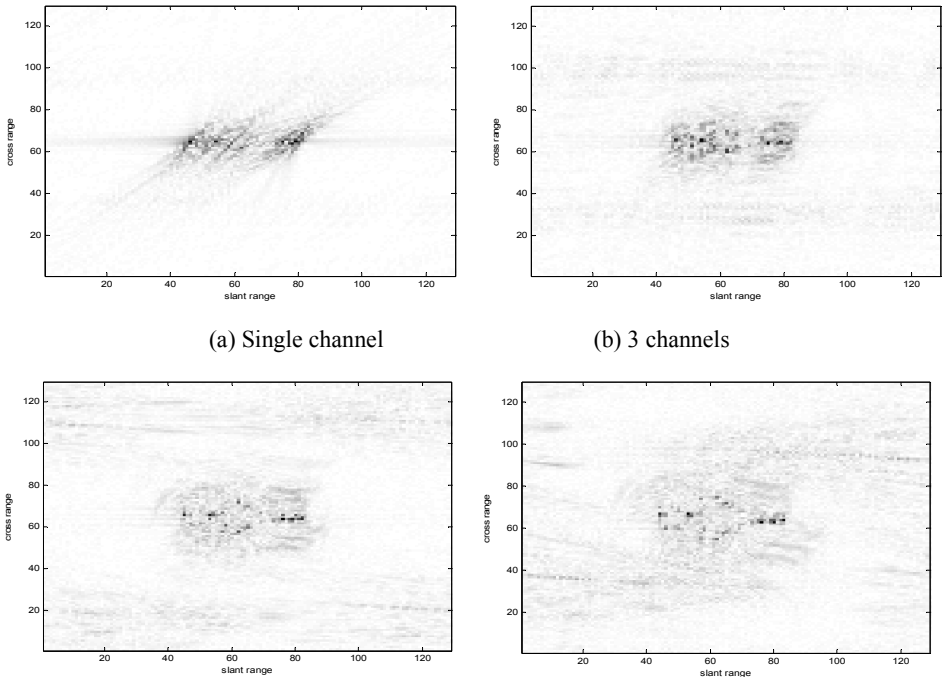

(a) Single channel (b) 3 channels

(c) 6 channels (d) 9 channels

Fig. 10. Polar coordinate reconstruction imaging.

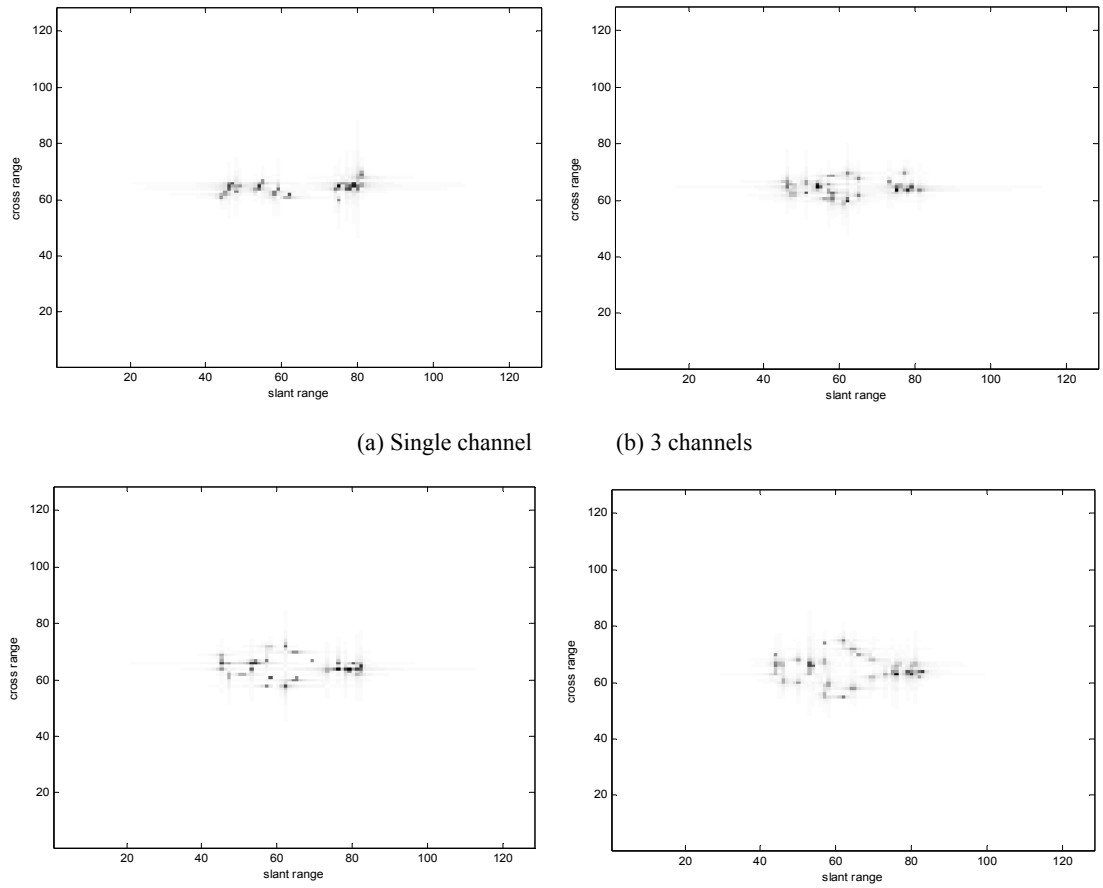

(a) Single channel (b) 3 channels

(c) 6 channels (d) 9 channels

Fig. 11. Imaging algorithm using PR-CLEAN.

6. Conclusion

In this paper, a method of passive ISAR imaging using multi-band DVB-T signals is studied. Firstly, the characteristics are analyzed as well as their ambiguity function of DVB-T and multi-channel DVB-T signals. Then, echo signal model is derived using multi-channel DVB-T signal under the single transmitter and multi receiver mode. At last, the PR-CLEAN imaging algorithm is introduced to image the target. Simulation results prove that the multi-channel DVB-T signals can be well applied in passive ISAR imaging, and the proposed algorithm based on PR-CLEAN can reduce the effect of interpolation operation, and result in better target images. The proposed analysis of multi-channel DVB-T signal and the PR-CLEAN imaging technology provide theoretical basis and research methods for the actual use passive ISAR imaging. The target imaging in this paper is studied in ideal conditions, and supposing the three synchronous, direct path interference processing suppression and motion compensation. In the further research, more factors based on external illuminator should be considered, especially the motion compensation problems in ISAR imaging, and then extend to the network-based ISAR imaging system using multi transmitter multi receiver modes.

Acknowledgements

The authors would like to thank the reviewers for their valuable and helpful suggestions.

References

[1]. Zhu Jia-Bing, Tao Liang, Hong Yi, Study on moving target detection to passive radar based on FM broadcast transmitter, *Systems Engineering and Electronics*, Vol. 18, Issue 3, 2007, pp. 462-468.

[2]. Shan Tao, Tao Ran, Wang Yue, et al., Study of detection performance of passive bistatic radars based on FM broadcast, *Systems Engineering and Electronics*, Vol. 18, Issue 1, 2007, pp. 22-26.

[3]. F. Belfiori, S. Monni, W. Van Rossum, et al., Antenna array characterization and signal processing for an FM radio-based passive coherent location radar system, *Radar, Sonar & Navigation*, Vol. 6, Issue 8, 2012, pp. 687-696.

[4]. Wang Hai-Tao, Wang Jun, L. Zhong, Mismatched filter for analogue TV-based passive bistatic radar, *Radar, Sonar & Navigation*, Vol. 5, Issue 5, 2011, pp. 573-581.

[5]. Wu Miao, Shan Tao, Zhuo Zhi-Hai, An adaptive filter with discrete distribution structure in DTV based passive radar, in *Proceedings of the 1st International Conference on Instrumentation,*

Measurement, Computer, Communication and Control, 21-23 October 2011, pp. 755-758.
[6]. Suwa Kei, Nakamura Shohei, Morita Shinichi, et al., ISAR imaging of an aircraft target USING ISDB-T digital TV based passive bistatic radar, in *Proceedings of the Geoscience and Remote Sensing Symposium (IGARSS)*, 2010, pp. 4103-4105.
[7]. Nakamura Shohei, Suwa Kei, Morita Shinichi et al., An experimental study of enhancement of the cross-range resolution of ISAR imaging using ISDB-T digital TV based passive bistatic radar, in *Proceedings of the Geoscience and Remote Sensing Symposium (IGARSS)*, 2011, pp. 2837-2840.
[8]. D. Olivadese, M. Martorella, E. Giusti, et al., Passive ISAR with DVB-T signals, in *Proceedings of the Synthetic Aperture Radar (EUSAR)*, 2012, pp. 287-290.
[9]. D. Olivadese, E. Giusti, D. Petr, et al., Passive ISAR with DVB-T signals, in *Proceedings of the IEEE Geoscience and Remote Sensing Society*, 2013, pp. 1-10.
[10]. Wang Da-Hai, Wang Jun, Research of passive radar imaging using single external illuminator and multiple receivers, *Chinese Journal of Electronics*, Vol. 34, Issue 6, 2006, pp.1138-1141.